Proceedings of ASME Turbo Expo 2021
Turbomachinery Technical Conference and Exposition
GT2021
June 7-11, 2021, Virtual, Online
GT2021-59844

THERMOACOUSTIC BEHAVIOUR OF A HYDROGEN MICROMIX AVIATION GAS TURBINE COMBUSTOR UNDER TYPICAL FLIGHT CONDITIONS

David Abbott*[1], Alessandro Giannotta[1], Xiaoxiao Sun[1], Pierre Gauthier[2], Vishal Sethi[1]

[1]School of Aerospace, Transport and Manufacturing, Cranfield University,
College Road, Cranfield, MK43 0AL, United Kingdom
[2]Siemens Energy,
9545 Cote de Liesse Road, Montreal QC H9P 1A5, Canada

ABSTRACT

Hydrogen micromix is a candidate combustion technology for hydrogen aviation gas turbines. The introduction and development of new combustion technologies always carries the risk of suffering from damaging high amplitude thermoacoustic pressure oscillations. This was a particular problem with the introduction of lean premixed combustion systems to land based power generation gas turbines.

There is limited published information on the thermoacoustic behaviour of such hydrogen micromix combustors. Diffusion flames are less prone to flashback and autoignition problems than premixed flames and conventional diffusion flames are less prone to combustion dynamics issues. However, with the high laminar flame speed of hydrogen, lean fuel air ratio (FAR) and very compact flames, the risk of combustion dynamics for micromix flames should not be neglected and a comparison of the likely thermoacoustic behaviour of micromix combustors and kerosene fueled aviation combustors would inform the early stage design of engine realistic micromix combustors.

This study develops a micromix combustor concept suitable for a modern three spool, high bypass ratio engine and derives the acoustic Flame Transfer Function (FTF) at typical engine operating conditions for top of climb, take-off, cruise, and end of runway. The FTF is derived using CFD and FTF models based on a characteristic flame delay. The relative thermoacoustic behaviour for the four conditions is assessed using a low order acoustic network code. The comparisons suggest that the risk of thermoacoustic instabilities associated with longitudinal waves at low frequencies (below 1kHz) is small, but that higher frequency longitudinal modes could be excited. The sensitivity of the combustor thermoacoustic behaviour to key combustor dimensions and characteristic time delay is also investigated and suggests that higher frequency longitudinal modes can be significantly influenced by combustion system design.

The characteristic time delay and thus FTF for a Lean Premixed Prevapourised (LPP) kerosene combustor is derived from information in the literature and the thermoacoustic behaviour of the micromix combustor relative to that of this kerosene combustor is determined using the same low order modelling approach. The comparison suggests that the micromix combustor is much less likely to produce thermoacoustic instabilities at low frequencies (below 1kHz), than the LPP combustor even though the risk in the LPP combustor is small.

It is encouraging that this simple approach used in a preliminary design suggests that the micromix combustor has lower risk at low frequency than a kerosene combustor and that the risk of higher frequency longitudinal modes can be reduced by appropriate combustion system design. However, more detailed design, more rigorous thermoacoustic analysis and experimental validation are needed to confirm this.

Keywords: Hydrogen; Micromix; Combustion; Thermoacoustics

NOMENCLATURE

Abbreviations

CFD	Computational Fluid Dynamics
EoR	End of Runway
FAR	Fuel Air Ratio
FDF	Flame Describing Function
FGM	Flamelet Generated Manifold
FTF	Flame Transfer Function
HP	High Pressure
IP	Intermediate Pressure
LES	Large Eddy Simulation
LH2	Liquid Hydrogen
LP	Low Pressure
LPP	Lean Premixed Prevapourised
OPR	Overall Pressure Ratio
PR	Pressure Ratio
RANS	The Reynolds-averaged Navier–Stokes
TET	Turbine Entry Temperature
ToC	Top of Climb

Latin Symbols

G	Temperature gradient with time
i	$\sqrt{-1}$
n	Flame transfer function gain constant
Q'	Fluctuating heat release
$\bar{Q}$	Mean heat release
t	Time
T	Temperature
u'	Fluctuating velocity upstream of the flame
$\bar{u}$	Mean velocity upstream of the flame

Greek Symbols

$\Delta\tau$	Spread of time delays
Θ	Flame transfer function parameter related to spread of time delays
τ	Characteristic or mean flame delay time
ω	Angular frequency
ξ	Flame transfer function gain constant related to Sauter mean diameter in liquid fuel flames

1. INTRODUCTION

The increasing concern over climate change and other environmental issues has led to ambitious emissions targets being imposed on the civil aviation industry, especially for CO_2 and NOx. In principle Liquid Hydrogen (LH2) used as an aviation fuel can result in zero carbon emissions at both mission and life cycle levels. The wide flammability limits of hydrogen allow lean combustion, potentially resulting in low NOx if an appropriate combustion technology can be developed. Cranfield University is coordinating the H2020 ENABLEH2 project [1] which is investigating a wide range of issues associated with the use of LH2 for civil aviation. A key part of the project is the investigation of an appropriate combustion technology and micromix combustion has been chosen.

Initially investigated for aviation applications by Aachen University [2, 3], including application to an Auxiliary Power Unit, hydrogen micromix employs many very small diffusion flames where air and fuel are mixed and burnt in a cross-flow pattern as illustrated in Figure 1.

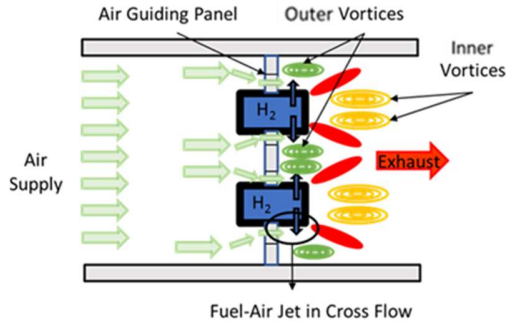

FIGURE 1: SCHEMA OF A TYPICAL HYDROGEN MICROMIX FLOW FIELD

This technology is based on the idea of minimizing the scale of mixing to maximize mixing intensity. The high-reactivity and wide flammability limits of hydrogen can produce short, low-temperature diffusion flames with lean overall equivalence ratios in a micromix combustor resulting in low NOx emissions.

The impact of injector design on NOx emissions is being actively investigated [4], [5], but an additional area of concern is the thermoacoustic behaviour of the combustor. The introduction and development of new combustion technologies always carries the risk of suffering from damaging high amplitude thermoacoustic pressure oscillation. This was a particular problem with the introduction of lean premixed combustion systems to land based power generation gas turbines. Diffusion combustors have historically been less prone to thermoacoustic issues than lean premix combustion and micromix is a diffusion combustion technology. However, key features of conventional diffusion combustors, such as relatively long diffuse flames and combustors with a significant number of dilution holes, are not present in micromix combustors. Thus, micromix may be more like lean premix combustion from a thermoacoustic perspective.

Ghirardo et al [6] conclude that flames with long time delays are more likely to excite thermoacoustic instabilities in a given combustor than those with shorter delays. This is encouraging as the intrinsically short micromix flames are likely to have short delays.

To investigate the likelihood of thermoacoustic instabilities causing problems in aviation applications of hydrogen micromix, this study develops a micromix combustor concept suitable for a modern three spool, high bypass ratio engine and derives the acoustic Flame Transfer Function (FTF) at typical engine operating conditions for top of climb (ToC), take-off, cruise, and end of runway (EoR). The FTF is derived using CFD and FTF models based on a characteristic flame delay. The relative thermoacoustic behaviour for the four conditions is assessed using a low order acoustic network code. The same methodology is used to assess the thermoacoustic behaviour of a kerosene Lean Premixed Prevapourised (LPP) combustor for the same application to allow the relative risk to be assessed.

2 PRELIMINARY COMBUSTOR DESIGN

2.1 Combustor operating conditions

In order to compare the behaviour of a kerosene combustor and a micromix combustor in an aviation setting, a typical three spool turbofan engine is modelled, to establish the gas properties at each stage of the engine. The following values of key parameters are chosen based on data for the Rolls-Royce Trent 1000 [7] as an example of its class:

- Net thrust at Take-Off equal to 309kN
- Net Thrust at Top of Climb equal to 68.5kN
- Bypass ratio equal to 10.7 at Top-of-Climb (chosen as Design Point condition)
- Maximum Turbine Entry Temperature (TET) equal to 1820K(at Take-Off)
- Overall Pressure Ratio at Design Point equal to 50

- Design-Point Inlet Mass Flow equal to 550kg/s

The performance of this representative three spool turbofan engine is calculated by a gas turbine performance code called TURBOMATCH developed by Cranfield University [8]. It requires an input file with the engine characteristics and the design point working conditions. In this paper, these parameters are selected according to typical turbofan engine characteristics reported in Walsh and Fletcher [9] and are summarised in Table 1.

TABLE 1: ENGINE WORKING CONDITIONS AT TOP OF CLIMB, DEFINED AS DESIGN POINT CONDITION FOR TURBOMATCH MODELLING

Altitude	9753.6m
Flight Mach number	0.82
Fan PR	1.54
Fan isentropic efficiency	0.915
By-pass ratio	10.7
IP compressor PR	8.12
IP compressor isentropic efficiency	0.87
HP compressor PR	4
HP comp. isentropic efficiency	0.87
HP Turbine cooling	18%
Burner Pressure Loss	5%
Combustion efficiency	0.9999
HP turbine isentropic efficiency	0.90
HP turbine Auxiliary work	500kW
IP turbine isentropic efficiency	0.91
LP turbine isentropic efficiency	0.93
Inlet Mass Flow	550kg/s
TET	1720K

At the design point, the TET is set at 1720K in order to meet the required thrust when kerosene is used. Then, the flight Mach number and the TET are assumed for the other flight conditions and the software calculates all the gas properties based on mass and energy balance. Firstly, the simulation is made setting the fuel as kerosene; then, the same engine is simulated switching the fuel to hydrogen. The results of the simulation are reported in Table 2. Using hydrogen at the same conditions as kerosene results in a higher thrust at every simulated operating condition because of several factors including the thermodynamic properties of the hot gas when hydrogen is burnt. In particular, a higher water content in the hot gas means that the gas entering the turbine has a higher constant-pressure specific heat, which results in lower turbine temperature drops (for delivering the same power), higher nozzle pressure ratio and higher thrust.

Since the engine must provide the same thrust when mounted on an aircraft, two possible strategies can be followed:

- increase the bypass ratio keeping the same TET;
- adjust the TET keeping the same bypass ratio.

Both have their advantages and disadvantages. If the bypass ratio is increased keeping the fan diameter constant, it generally increases the propulsive efficiency, but the reduced size of the core can have an impact on the isentropic efficiencies of the engine components. If the bypass ratio is kept equal, the TET must be reduced resulting in a lower thermal efficiency and thus only a partial exploitation of the current technology capabilities.

Therefore, the first strategy is followed in this work and the results are shown in Table 3.

TABLE 2: COMPARISON OF PERFORMANCE RESULTS BETWEEN HYDROGEN (IN GREEN) AND KEROSENE (IN YELLOW) WITH THE SAME BYPASS RATIO

	ToC		Take off		Cruise		EoR	
Altitude (m)	9753.6		0		10668		0	
Mach Number (-)	0.82		0		0.85		0.25	
TET (K)	1720		1820		1620		1750	
OPR (-)	50	50	45.53	45.17	44.12	55.53	39.65	39.59
Inlet Mass Flow (kg/s)	550	550	1152.2	1137.7	477.4	479.14	1139.5	1127.8
Bypass Ratio (-)	10.7	10.7	10.7	10.6	11.5	11.4	11.47	11.36
Fuel Mass Flow (kg/s)	0.3783	1.002	0.8405	2.1976	0.2817	0.7565	0.7282	1.9238
Thrust (kN)	71.85	68.52	323.15	308.63	53.71	51.64	215.8	204.72

TABLE 3: COMPARISON OF PERFORMANCE RESULTS BETWEEN HYDROGEN (IN GREEN) AND KEROSENE (IN YELLOW) WITH DIFFERENT BYPASS RATIO, DELIVERING THE SAME DESIGN POINT THRUST

	ToC		Take off		Cruise		EoR	
Altitude (m)	9753.6		0		10668		0	
Mach Number (-)	0.82		0		0.85		0.25	
TET (K)	1720		1820		1620		1750	
OPR (-)	50	50	45.55	45.17	44.06	44.53	39.6	39.59
Inlet Mass Flow (kg/s)	550	550	1145.3	1137.7	477.3	479.14	1130.9	1127.8
Bypass Ratio (-)	11.55	10.7	11.4	10.6	12.5	11.4	12.29	11.36
Fuel Mass Flow (kg/s)	0.3526	1.002	0.7834	2.1976	0.2623	0.7565	0.6783	1.9238
Thrust (kN)	68.52	68.52	313.12	308.63	50.899	51.64	206.37	204.72

2.2 Combustor geometries

Typical dimensions of an engine with the above design parameters are derived from diagrams given in [10], assuming a fan diameter of 2.80m [7]. These are used to define the available combustor space envelope. Combustor geometries for both a kerosene combustor and a micromix combustor are then developed.

For the kerosene combustor, the preliminary design methodology is based on Mellor [11] and Mattingly et al. [12]. For the micro-mix combustor, the same preliminary design methodology is followed, however the intrinsic differences between kerosene and hydrogen and micromix combustors are significant and the following have to be considered:

- one of the most distinctive characteristics of the micro-mix combustor systems is the absence of primary, secondary and dilution zones. Hence, the passage between the combustor has to pass significantly less air and can be reduced.
- For simplicity, both the combustors have the same film cooling technology.
- In kerosene combustors there are typically of the order of 10 discrete burners. In the micromix combustor these are replaced by thousands of micro-injectors The number of injectors is chosen based on the micro-injector geometry, its desired inlet velocity and the total air mass flow passing through them.

- Although hydrogen generally produces shorter flames than kerosene, the combustor length is kept the same, in order to fit the same engine. The same applies to the combustor casing. In engines designed specifically for micromix, the combustor and thus shaft length could be significantly reduced.
- The pre-diffuser of the micro-mix combustor is kept equal to the kerosene combustor. However, as the amount of passage flow is reduced and the dome height increased, the pressure losses in the diffuser are higher.

CAD models reproducing one twelfth of the annuli of the resulting combustors are shown in Figure 2 and Figure 3. These geometries form the baseline for the thermoacoustic analysis.

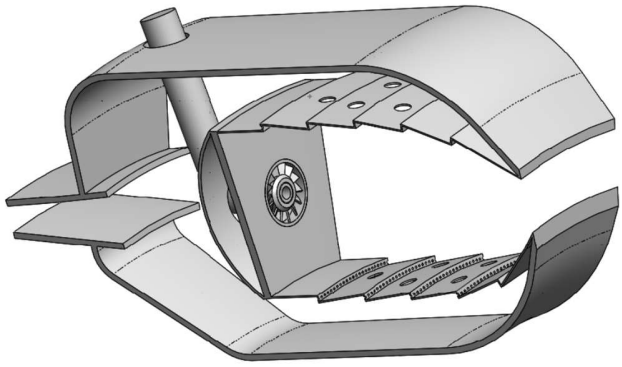

FIGURE 2: CONVENTIONAL COMBUSTOR CAD MODEL OBTAINED BY A PRELIMINARY DESIGN METHODOLOGY.

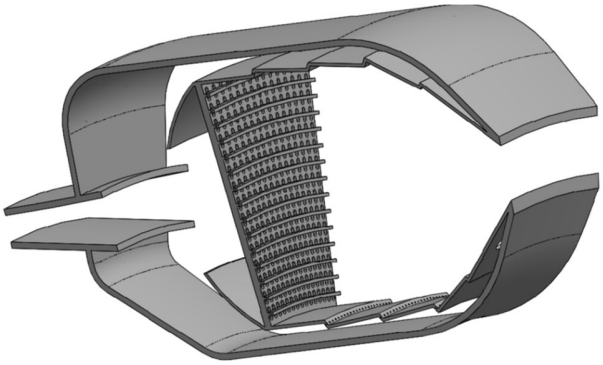

FIGURE 3: MICROMIX COMBUSTOR CAD REPLACING THE CONVENTIONAL COMBUSTOR.

3 APPROACHES TO THERMOACOUSTIC ANALYSIS

Poinsot [13] describes the possible approaches to the thermoacoustic analysis of gas turbine combustors. These are summarised in Figure 4. This shows two main approaches: the first of which Poinsot refers to as "Brute Force LES" and requires the solution of full 3D Navier-Stokes equations by transient Large Eddy Simulations. To achieve this the model must include all parts of the geometry that could influence the acoustic behaviour of the system and define appropriate boundary conditions. For a typical aviation gas turbine combustor this would require a model including all the geometry and flow paths between the compressor discharge and the turbine inlet which results in an extensive model requiring transient solution over a significant time period. Thus, although this strategy can give a detailed understanding of the thermoacoustic behaviour, the computational costs are high, making early stage design evaluation and sensitivity analysis impractical.

This approach does not require any acoustic code and the acoustic perturbations are self-excited by the transient combustion behaviour as in the real situation. Thus, this method may be referred to as the "Self-Excited Method". Because of the desire to perform early stage design and sensitivity analysis, this approach will not be considered further in this paper, but will be considered in future for more detailed assessments.

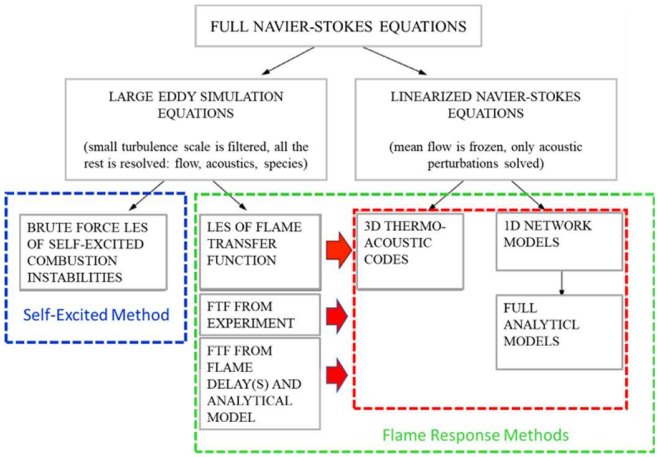

FIGURE 4: APPROACHES TO THERMOACOUSTIC ANALYSIS (AFTER [13])

The second approach, referred to here as the "Flame Response Method", significantly reduces the computational costs. The flame acoustic characteristics are modelled or measured separately and incorporated into a separate acoustic code modelling the acoustics of the combustor geometry. The flame may be represented by a Flame Transfer Function (FTF) as described by Andreini et al [14], but the FTF is restricted to small perturbations and cannot be used to predict limit cycle oscillation amplitudes or other non-linear effects [15] and a non-linear Flame Describing Function (FDF) may be defined. This effectively describes the FTF as a function of inlet disturbance amplitude. This paper only considers the linear FTF and this limits the analysis to the identification of the occurrence of unstable modes together with their frequency and initial growth rate. The limit cycle oscillation amplitude will not be determined.

For the purposes of this study an open source thermoacoustic network modelling code developed by Prof. Morgans and co-workers at Imperial College [16] is used as the low order code.

4 FLAME TRANSFER FUNCTION

The classic definition of the FTF is given by [14]:

$$FTF(\omega) = \frac{Q'/\bar{Q}}{u'/\bar{u}} \quad (1)$$

where Q' and $\bar{Q}$ are the fluctuating heat release and mean heat release respectively and u' and $\bar{u}$ are fluctuating and mean velocity upstream of the flame respectively.

As indicated in Figure 4 the FTF may be determined by experiment, LES modelling or the use of analytical models. FTFs for a micromix flame determined by both LES modelling and the use of analytical models and RANS CFD have been reported by McClure [17] and Cranfield University is currently developing test rigs to investigate micromix combustion characteristics over a wide range of operating conditions, including the measurement of the FTFs, but this data is not available for this study.

Simple analytical models of the FTF using characteristic flame delay times determined from RANS CFD have a significant analysis time advantage over LES methods for determining the FTF and are thus convenient to use during early stage design. The first analytical model was the n-τ model proposed by Crocco [18] and the FTF is given by [14]:

$$FTF_1(\omega) = -ne^{-i\omega\tau} \quad (2)$$

where n is a constant representing the gain of the flame response and τ is a characteristic time delay for the flame.

This formulation has proved useful as it provides a good representation of the behaviour of many flames, particularly at low frequency. Several improvements to the basic n-τ model have been proposed to account for the fact that there may be a spread of characteristic delay times within a real flame. A model proposed by Sattelmeyer and Eckstein [19] [20] and discussed in [14] characterises the time delay as a mean time delay τ and a range of delays of ±Δτ evenly distributed about this mean (i.e. a top-hat distribution is assumed). This results in a modified FTF of:

$$FTF_2(\omega) = -n\Theta e^{-i\omega\tau} \quad (3)$$

where Θ represents the effect of the spread of time delays and is given by:

$$\Theta = \frac{\sin(\omega\Delta\tau)}{(\omega\Delta\tau)} \quad (4)$$

For liquid fuel the mechanisms may be different and Andreini [14] reports the following form derived by Eckstein for diffusion flames with an air blast atomiser:

$$FTF_3(\omega) = 2\xi\Theta e^{-i\omega\tau} \quad (5)$$

where ξ is a constant that depends on the Sauter mean diameter of the droplet population. A similar form of transfer function was used by Cheung et al [21] to fit a measured FTF of a kerosene LPP combustor.

5 LOW ORDER MODELLING

For this study the open source code OSCILOS is chosen. OSCILOS comes in two forms OSCILOS_long and OSCILOS_ann. The former is a 1-D code only allowing the analysis of longitudinal modes whereas the latter is a 2-D allowing the analysis of both plane/circumferential waves that may be present in annular combustors [16].

OSCILOS_ann models typical annular combustion systems as two annular spaces representing compressor discharge plenum and combustor connected by a finite number of axial connections representing the burners. However, because micromix combustion consists of a very large number of very small flames the impact of the spatial distribution of the burners on the eigenmodes will be very different in micromix which will act as a distributed flame. Thus, further development of the code is needed before the circumferential behaviour of micromix can adequately be modelled using OSCILOS. However, the longitudinal behaviour can be modelled using OSCILOS_long and this has been undertaken as an indication of the thermoacoustic behaviour of micromix combustion.

In OSCILOS-long, combustor geometries are represented by a network of cylindrical tubes with different cross-sectional areas. The longitudinal modes of an annular combustor can be modelled by representing the annular components as a series of cylinders of the same axial length and same open cross-sectional area as the annular components. The axial connections through the micromix burners are represented as a single cylinder of the same length and total open cross-sectional area as the micromix injectors. The code allows the flame to be modelled by linear FTFs or non-linear FDFs, either derived analytically within the code from characteristic time delays or loaded from external data files. External data files can contain FTFs or FDFs derived from more complex analytical models, experimental or CFD data.

Full details of the acoustic theory behind the code are contained in the OSCILOS Technical Report [22].

6 CFD MODEL SETUP

The objective of this CFD analysis is to derive a set of FTFs for hydrogen micro-mix combustor flames. In this work, a single injector is considered, based on the most recent injector design exploration at Cranfield University [4] which aims to minimise NOx emissions. The software used for the analysis is STAR-CCM+. The fluid region of the single injector with the boundary definitions are shown in Figure 5.

All the simulations are performed using a 3-D steady RANS approach coupled with the $k-\omega$ SST turbulence scheme, while the combustion is modelled by the Flamelet Generated Manifold (FGM) model. Based on the work done by Lopez et al. [23], the following non dimensional numbers are selected to define hydrogen combustion:

- Schmidt number equal to 0.25
- Turbulent Schmidt number equal to 0.2

The fluid region is meshed with polyhedral mesh and Prism Layer mesh in the proximity of wall-type boundary conditions to capture the boundary layer. The average y^+ across all wall surfaces downstream of the air gate is kept below 3.

The grid independency is tested on three different grids: coarse, medium and fine mesh of about 0.7, 1.2 and 2 million cells, respectively. The medium mesh with a base size of 0.75mm

is selected for all the simulations after it demonstrated good agreement with the fine mesh results.

The operating conditions of the single injector are derived from the turbofan performance analysis described in Section 2.1 and are given in Table 4.

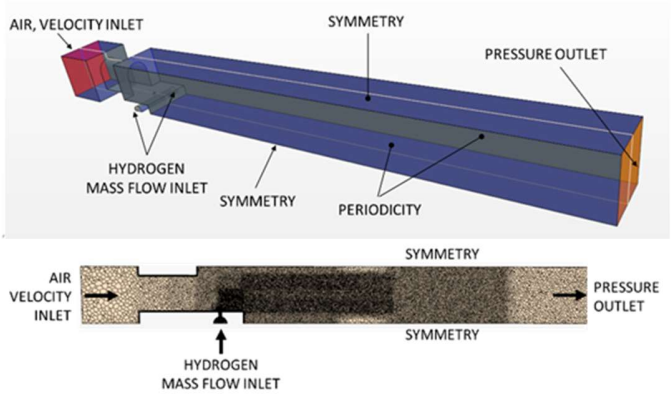

FIGURE 5: FLUID REGION OF A SINGLE INJECTOR WITH BOUNDARY DEFINITIONS (TOP) AND MESH (BOTTOM)

TABLE 4: COMBUSTOR OPERATING CONDITIONS

	ToC	Take-Off	Cruise	EoR
TET (K)	1720	1820	1620	1750
Inlet Velocity (m/s)	16.00	16.84	15.57	16.66
Operating Pressure (Bar)	21.35	46.15	16.84	41.92
Equivalence ratio, Φ	0.421	0.446	0.386	0.417
T_{air} (K)	851.6	922.7	805.8	896.8
T_{H_2} (K)	600	600	600	600
Air mass flow (kg/s)	1.041	2.187	0.845	2.022

7 RESULTS

7.1 CFD

Figure 6 shows the mean total temperature field on the centre plane of the region for the four flight conditions. The results at all operating conditions show good positioning of the flame near the edge of the hydrogen injection point. Micromix technology aims to exploit the presence of two recirculation zones (symbolically shown by two red circles in the Take-Off case in Figure 6) to burn the fuel in a thin shear layer between these vortices, thus avoiding fuel concentration and high-temperature peaks [5]. The cruise case has a shorter flame and a lower maximum total temperature, as the fuel mass flow is lower at cruise conditions.

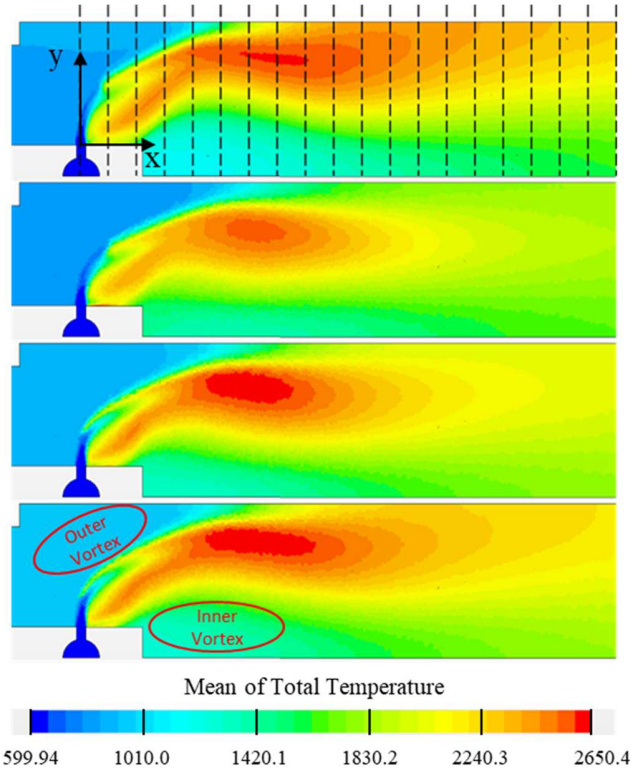

FIGURE 6: TEMPERATURE CONTOURS AT MIDDLE CROSS SECTION SHOWING AVERAGING PLANES. FROM TOP TO BOTTOM: TOC, CRUISE, EOR, TAKE-OFF. (x is the axial direction and direction of mean flow, y is the radial direction and the circumferential direction is into the page)

7.2 Flame Transfer Functions

7.2.1 FTF for Micromix combustion

In order to use equations 2 or 3 values of n, τ and $\Delta\tau$ are required. As the FTF is a normalised quantity, it may be assumed that n=1 based on the quasi-steady assumption that at low frequency $\left|\frac{Q'}{u'}\right| = \left|\frac{\bar{Q}}{\bar{u}}\right|$, thus the low frequency limit is $\left|\frac{Q'/\bar{Q}}{u'/\bar{u}}\right| = 1$. This value is used for all the operating conditions considered.

To determine the flame transfer function for each operating condition, estimates of the delay (τ) and spread of delays ($\Delta\tau$) must be determined. The estimation of the time delay from steady state information provided by RANS CFD, effectively limits the possible delays to convective times within the flame. The most common method of determining the time delay is to assume that the relevant time delay is the time from fuel injection to the flame front [17], [24], [25], [26] and to track particles from fuel injection to the flame front. This requires an assumption as to what constitutes the flame front. It is usual to define the flame front as an iso-surface of an appropriate parameter such as remaining fuel mass fraction [25], reaction progress variable [24], [17] or maximum heat release [26] and some assumption has to be made about the appropriate value of the chosen parameter.

For this study an alternative approach to determining the time delay from RANS is proposed. As with the particle injection method described above, it is assumed that the appropriate time delay is the time from fuel injection to combustion. However, considering longitudinal plane waves in the combustor, these waves are influenced by planar average conditions as they propagate along the combustor rather than the detailed distribution of conditions over the plane, thus considering planar averages would be appropriate. The flame amplifies the acoustic wave due to the volume velocity increase it produces. The increased volume flow under lean conditions is principally due to the expansion caused by the increase in temperature.

Considering the quasi-steady situation, the first volume expansion experienced by the incoming flow is when the temperature increases, either due directly to local heat release or due to mixing processes. When considering planar (mass weighted) averages the rise from one plane to the next is representative of the progressive increase in volume experienced by the flow.

In the proposed method planar mass weighted average temperatures are determined at a number of planes throughout the combustion zone as indicated in the top image of Figure 6. Similarly, the area weighted average velocity is determined at each plane to enable plots of temperature against distance to be converted to plots of temperature against mean time from fuel injection. This results in plots of the form shown in Figure 7.

If the gradient of the temperature (i.e. temperature rise) representing combustion is plotted against time, this results in Figure 8, representing the time delay from fuel injection to combustion. It can be seen in Figure 8 that the temperature rise starts almost immediately after fuel injection with no significant delay before combustion. Thus, to approximate the top hat distribution assumed in FTF $_2$ the centre of the distribution is determined by the mean delay (τ). To have the start of distribution (i.e. $t = \tau - \Delta\tau$) with a non-negative value of time $\Delta\tau$ is taken as numerically equal to τ as illustrated in Figure 8. (Generally, if there is a delay before the start of combustion τ will be greater than $\Delta\tau$.) For this study, τ and $\Delta\tau$ were determined as follows:

Taking the gradient G_j at time t_j to be

$$G_j = \frac{T_{j+1} - T_{j-1}}{t_{j+1} - t_{j-1}} \qquad (6)$$

where T is the temperature and t is time.

Then τ and $\Delta\tau$ is given by the weighted average time delay:

$$\tau = \Delta\tau = \frac{\sum(G_j t_j)}{\sum G_j} \qquad (7)$$

This results in the time delays and spreads as shown in Table 5. It should be noted that in this case the mean delay and spread of delays are the same because some combustion (thus temperature rise) occurs close to the fuel injection. In general, this will not be the case and thus both are quoted.

Table 5: TIME DELAYS FOR MICROMIX COMBUSTION

Condition	Mean delay, τ (ms)	Spread of delays, $\Delta\tau$ (ms)
Top of Climb	0.156	0.156
Take-off	0.142	0.142
Cruise	0.155	0.155
End of Runway	0.144	0.144

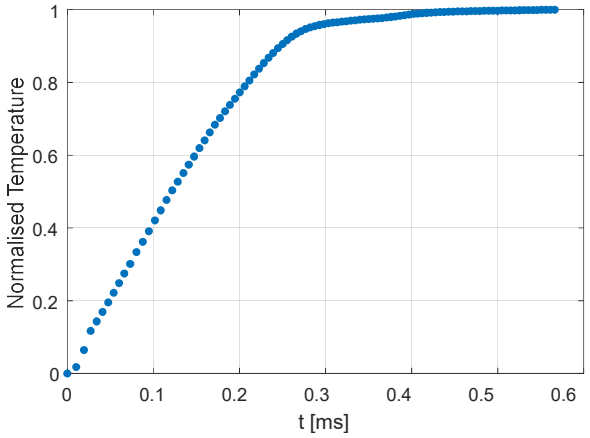

Figure 7: MEAN TEMPERATURE AGAINST MEAN PROPAGATION TIME FOR THE EoR CASE

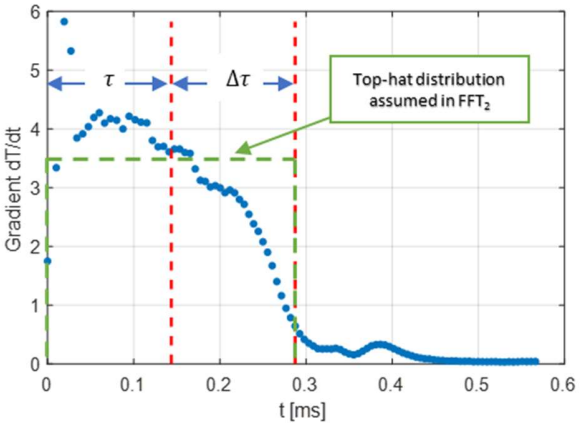

Figure 8: GRADIENT CALCULATED WITH A CENTRAL FINITE DIFFERENCE SCHEME AGAINST MEAN PROPAGATION TIME FOR THE EoR CASE

7.2.2 FTF for conventional kerosene combustion

It is not within the scope of this study to perform CFD analysis of a kerosene combustor to determine characteristic time delays. Measured FTFs are sought in the literature. Cheung et al [21] reported measurements of the FTF for Lean Premixed Prevapourised (LPP) kerosene combustion. As LPP combustion is a low NO_X kerosene technology it is considered appropriate to compare this with micromix as an alternative low NO_X combustor. Cheung et al measured a range of conditions including those representing HP Idle, Approach and Take-off, together with atmospheric tests. They also fit a function of the

same form as FTF $_3$ (Equation 5) to the atmospheric test data. For this study a revised fit to all the data in [21] is made and taken as representative of all conditions (Figure 9) for this study.

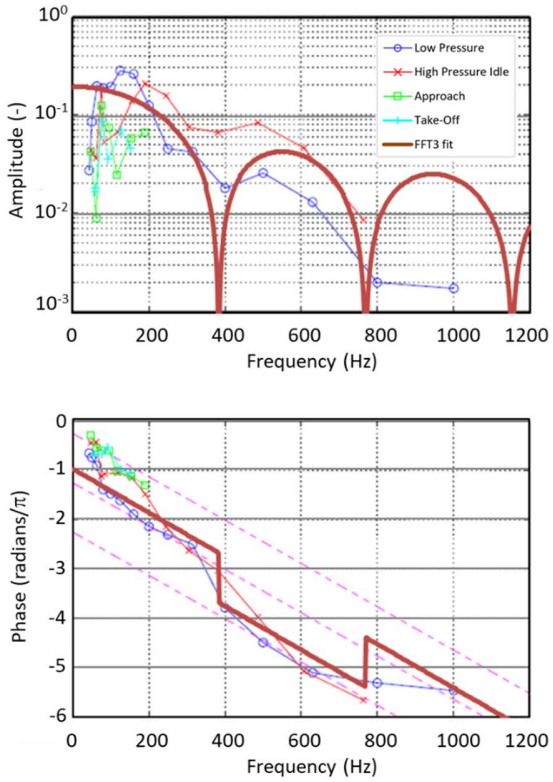

FIGURE 9: FTF DATA FOR LPP COMBUSTION FROM [21] WITH FTF $_3$ FIT

7.3 Eigenmodes

The longitudinal eigenmodes for a range of cases are determined using OSCILOS_long, based on the geometries (converted to equivalent cylinders) and the operating conditions described in Sections 2.1 and 2.2. The geometry inputs to OSCILOS are shown in Figure 10.

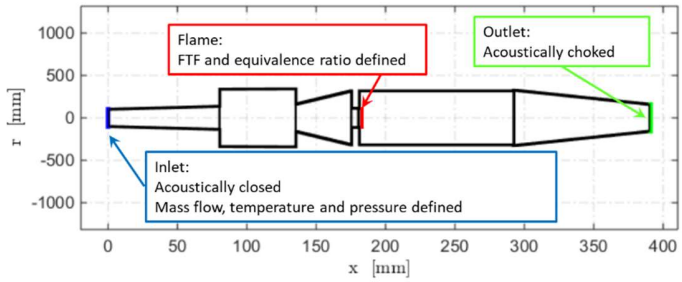

FIGURE 10: SCHEMA OF OSCILOS SET UP

This analysis uses linear FTFs to characterise the flame response and in this case the main output from OSCILOS is a list of the eigenmodes together with their frequency and growth rate. Modes with negative growth rates are decaying modes and do not produce high amplitude thermoacoustic pressure oscillations. For modes with positive growth rates, pressure oscillations grow until non-linear effects limit further growth. Mode shapes are also available allowing locations of highest acoustic pressure to be identified.

It should be noted that this analysis only considers longitudinal modes of the combustor. Above the frequency for circumferential mode formation, circumferential, axial and mixed modes will be possible in the real combustor. Above the frequency for radial (cross) modes, radial and further mixed modes will be possible. For the conditions considered, the frequencies of the first circumferential and radial modes are approximately 425Hz and 2700Hz respectively.

The simple n-τ model (FTF $_1$) would in many cases be simpler to use in early stage design and the effect of using this rather than the more representative modified n- τ model (FTF $_2$) is investigated for the ToC case. Figure 11 shows a plot of growth rate and frequency for the eigenmodes determined using OSCILOS; positive growth rates indicate unstable modes and negative growth rates indicate stable modes. It can be seen that similar eigenfrequencies occur in both cases, but as may be expected, the growth rate is lower, particularly at higher frequencies for the modified n- τ case because the magnitude of the gain is lower at high frequencies for FTF $_2$. Use of FTF $_1$ thus results in overpredicting the risk of high amplitude thermoacoustic pressure oscillation. This conservative approach may be acceptable for early design investigations.

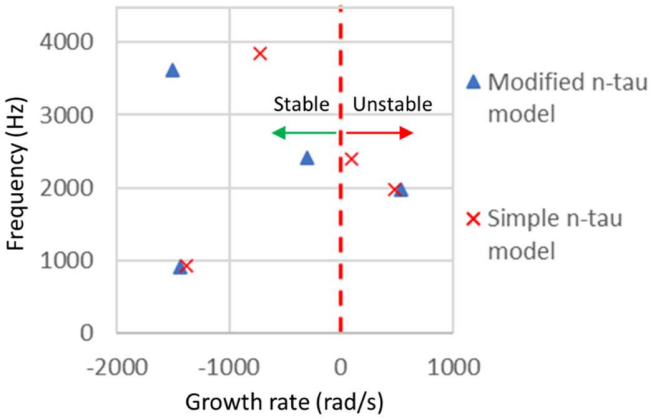

FIGURE 11: COMPARISON OF EIGENMODES FOR TOC DETERMINED USING SIMPLE N- τ MODEL (FTF $_1$) AND MODIFIED N-τ MODEL (FTF $_2$)

The simple linear approach taken in this study does not allow the amplitude of limit cycle oscillations to be determined and any positive growth rate could result in very high amplitude oscillations. The final limit-value amplitude will depend on non-linear effects. Similarly, high growth rate does not necessarily lead to very high amplitudes as non-linear effects may prevent significant growth and limit the oscillation to non-damaging amplitudes. However, from an early design perspective, all positive growth rates are undesirable as damaging oscillations

could occur and higher growth rates are likely to be more problematic as greater measures (e.g. increased acoustic damping) will be needed to suppress these modes.

The eigenmodes for the micromix combustor are determined for all the operating conditions using FTF $_2$ with τ and $\Delta\tau$ as in Table 5. It can be seen (Figure 12) that the thermoacoustic behaviour is predicted to be similar for all cases with unstable longitudinal modes at about 2kHz.

A comparison of the micromix and kerosene LPP combustors is made using the ToC value of FTF $_2$ for micromix and the FTF$_3$ fit shown in Figure 9 for kerosene together with the appropriate geometries for each case. The analysis was only performed up to 1.2kHz as the FTF data for the kerosene flame was only available in this frequency range (Figure 9). Figure 13 shows that in this frequency range both combustion systems are predicted to have no unstable longitudinal modes. The micromix combustor has only one predicted mode in this region and this has a lower growth rate than any of the modes for the LPP combustor.

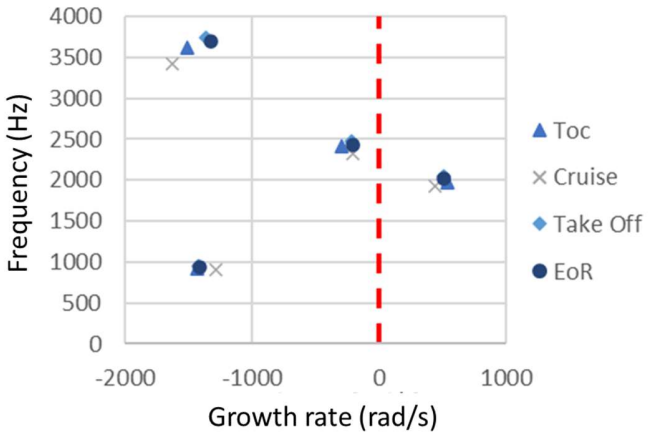

FIGURE 12: COMPARISON OF EIGENMODES FOR ALL MICROMIX CASES

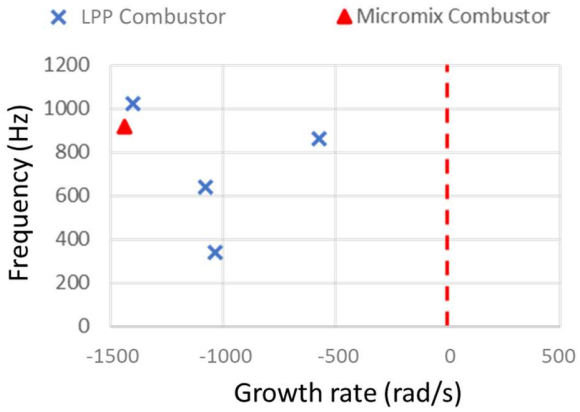

FIGURE 13: COMPARISON OF EIGENMODES FOR MICROMIX AND LPP KEROSENE COMBUSTORS (ToC CASE)

7.4 Sensitivity analysis

In the early stages of combustor design, it is particularly useful to evaluate the effect of key design dimensions. The sensitivity of the eigenvalues to key geometrical features is investigated.

The parameters varied (Figure 14) are pre-diffuser length (L1), dump gap between the pre-diffuser and the cowl inlet (L2), the distance from the cowl inlet to the injector-plate (L3), the thickness of the injector plate (L4), the length of the non-converging section of the combustor (L5) and the dome height (H1). The length of the converging section of the combustor (L6) is varied to keep the sum of L1 to L6 constant as this length is dictated by the engine architecture. In this study the effect of changing more than one parameter at a time was not assessed.

ToC conditions are used as representative and the simple n-τ model is used.

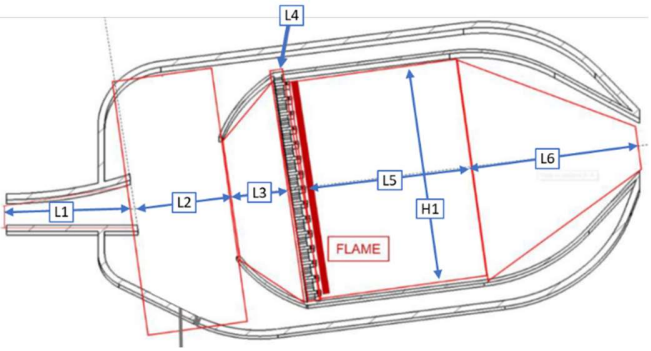

FIGURE 14: COMBUSTOR GEOMETRY SHOWING DIMENSIONS VARIED IN THE SENSITIVITY ANALYSIS

Dome height (H1) is varied from 113 to 155mm and no change in the eigenvalues is seen. This is not surprising as this height has only minimal effect on the longitudinal waves in the combustor through the relatively small change in mean axial velocity.

Pre-diffuser length (L1) is increased in steps from 60mm to 140mm. It can be seen (Figure 15) that this has a significant impact on the eigenvalues with the unstable mode at 1.985kHz progressively decreasing in both frequency and growth rate. The greatest lengths significantly suppress this mode, but another higher frequency unstable mode at between 2 and 3 kHz appears.

This clearly shows the potential impact of pre-diffuser length on the thermoacoustic behaviour of the system and its potential to affect the risk of undesirable pressure oscillations. However, in this case this may be due to the change in combustor length (L5 + L6) that occurs to maintain the overall system length constant.

The length of the pre-diffuser to cowl gap (L2) is varied from 30 to 60mm (Figure 16(a)). Increasing the gap from 30 to 40mm decreases the growth rate of the most unstable mode (about 2kHz), but increasing L2 further (to 50 and 60mm) progressively increases the growth rate again, suggesting that there is an optimum value of L2.

The length of the cowl (L3) is varied from 5 to 35mm and has no significant impact on the unstable mode at about 2kHz

(circled in Figure 16(b)), but other modes are affected, thus the impact of L3 cannot be ignored.

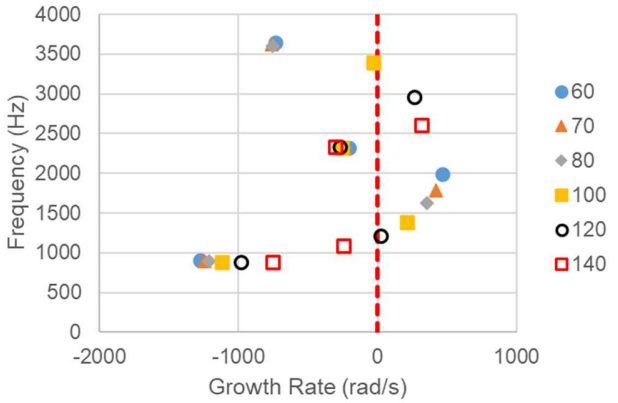

FIGURE 15: EFFECT OF L1 (PRE-DIFFUSER LENGTH) ON EIGENVALUES (ToC)

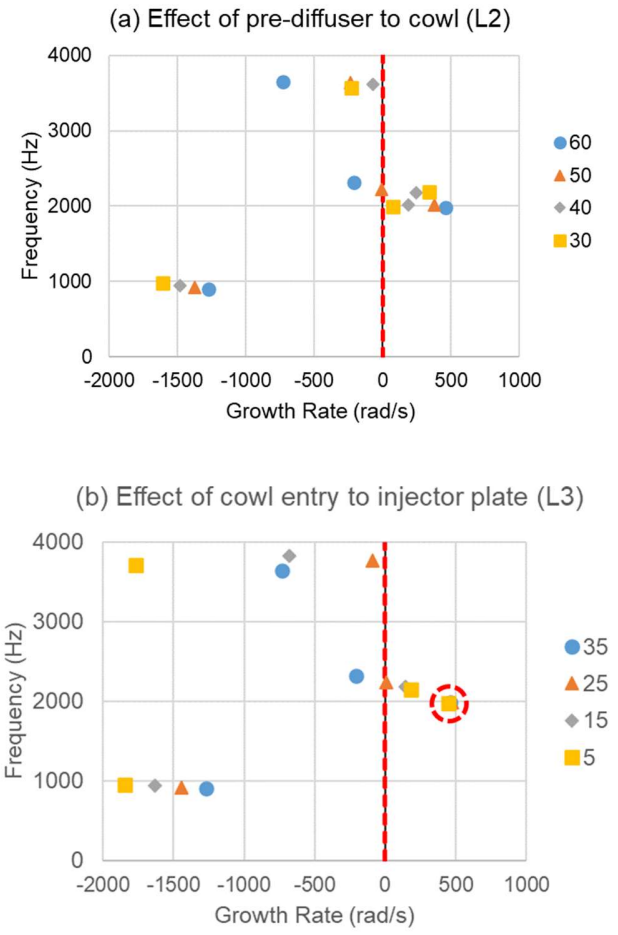

FIGURE 16: EFFECT OF LENGTHS L2 AND L3 UPSTREAM OF INJECTOR PLATE ON EIGENVALUES (~2kHz mode circled)

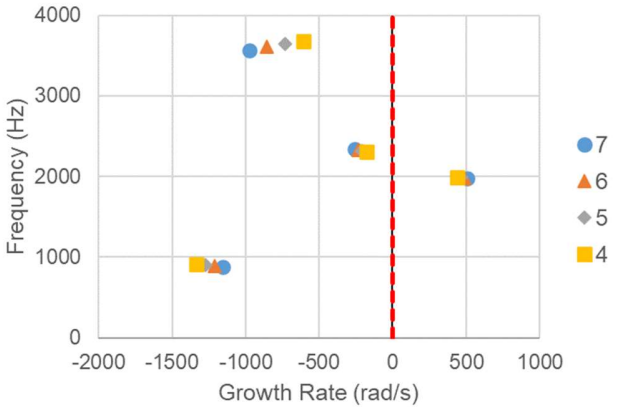

FIGURE 17: EFFECT OF L4 (INJECTOR PLATE THICKNESS) ON EIGENVALUES.

The injector thickness (L4) is varied from 4 to 7mm (Figure 17). This produces clear trends in the observed eigenvalues. Decreasing L4 slightly decreases the growth rate of the unstable mode at about 2kHz, but the growth rate of the stable mode at about 900Hz decreases significantly. This also increases the growth rate of the stable modes at about 2.3 (slightly) and 3.6kHz (significantly).

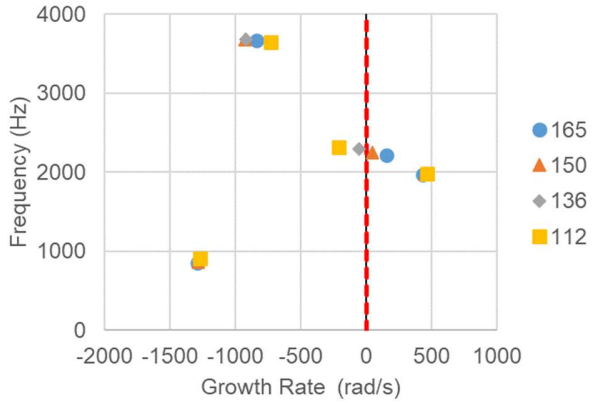

FIGURE 18: EFFECT OF (L5) NON-CONVERGING COMBUSTOR LENGTH ON EIGENVALUES

The non-converging combustor length (L5) is varied from 112 to 165mm. This has very little impact on the growth rate of the most unstable mode at about 2kHz (Figure 18). This may be surprising but the total length L1 to L6 is kept constant by varying L6, thus the combustor length (L5 + L6) is constant. The impact on the other eigenmodes seen in Figure 18 is due to the effect of varying the balance between the constant cross section (L5) and reducing cross section (L6) parts of the combustor.

This shows that geometric changes can significantly affect the longitudinal mode frequencies and growth rates and thus the risk of problematic pressure oscillations. However, individual

features cannot be identified as more critical than others due to the interaction between the lengths L1 to L6 and the influence these have on the acoustic properties of the system and the positioning of the flame within that system.

8 DISCUSSION

The CFD analysis shows that hydrogen micromix is characterised by short time delays: This is not surprising because this is part of the design intent to produce low NO_X emissions. However, characteristic delay times are found to be an order of magnitude less than those for kerosene flames. Because of this higher frequency eigenmodes would be expected to be favoured. This is seen in the eigenmode analysis where no longitudinal modes are seen below 800Hz.

Comparison with kerosene LPP (Figure 13) shows that for the chosen geometry, in the frequency range analysed, several modes exist for kerosene, but they are all stable. Only a single mode is seen for micromix and this has a lower growth rate than any kerosene mode. Thus, for the geometries chosen, hydrogen micromix will have a lower risk of problematic thermoacoustic pressure oscillation due to longitudinal modes up to about 1kHz than a kerosene LPP combustor under similar duties. This is encouraging, but the higher frequency modes are of concern and require further investigation.

A separate paper [27] investigates the relationship between FTFs derived from RANS and LES approaches for micromix. LES results suggest that the phase of the FTF is well represented by the RANS approach, but that the RANS approach over-estimates the gain at high frequency. If future planned experimental determination of the FTF confirms the LES finding the risk of high frequency thermoacoustic issues will be less than indicated by this study.

The sensitivity analysis shows that the geometry can be optimised to reduce growth rates of the higher frequency longitudinal modes and thus risk of problematic thermoacoustic pressure oscillations. However, the analysis to date is not sufficient to conclude whether risk can be fully mitigated without recourse to specific acoustic damping measures.

Operating conditions do not show a significant impact on the predicted behaviour because the FTFs were similar for each case. This suggests that any acoustic control measures (geometry optimisation or added acoustic dampers) are likely to be effective over the full operating range, but this requires confirmation.

The analysis was limited to longitudinal modes and analysis of circumferential and radial modes is needed. The short time delays suggest that higher frequencies may also be favoured for these modes. In particular radial modes are likely to be of particular interest due to their higher frequency nature (shorter characteristic lengths).

Development of the network modelling approach is needed to be able to accommodate the thousands of individual injectors distributed both radially and circumferentially and to assess the impact on both circumferential and radial modes. Radial and circumferential staging (i.e. the variation of fuel input to individual injectors) may be used to control the exit temperature profile, improve turndown characteristics and possibly for the control of thermoacoustics. Future developments in the modelling approach need to be able to assess the impact of staging.

Better estimates of the FTF (ideally FDF) are needed to confirm and/or improve the simple FTF models used. Currently, work is underway to determine micromix FTFs using LES and to measure them experimentally.

9 CONCLUSIONS

A new method of determining the characteristic flame time delay and spread of delays is proposed and used to determine the FTF for micromix combustion. This method requires validation by experimental measurement, but has proved useful in the preliminary design studies of a hydrogen micromix combustor.

The FTF together with acoustic network analysis indicates that micromix is significantly less likely to produce low frequency (below 1kHz) thermoacoustic oscillations due to longitudinal modes than a kerosene LPP combustor. At higher frequencies longitudinal modes could be excited, but the risk can be significantly reduced by optimising the combustion system design. Further consideration of circumferential and radial modes is required to assess the overall thermoacoustic behaviour of micromix combustors.

Further work is required on both the determination of the FTFs and the thermoacoustic system models to confirm these results and to undertake more detailed thermoacoustic design. These thermoacoustic models need to be able to describe the distributed nature of the thousands of individual injectors and be able to accommodate both radial and circumferential modes and staging.

ACKNOWLEDGEMENTS

The ENABLEH2 Project is receiving funding from the European Union's Horizon 2020 research and innovation programme under grant agreement Nº 769241.

REFERENCES

[1] European Commission. (2018). ENABLing cryogEnic Hydrogen based CO2 free air transport (ENABLEH2). https://cordis.europa.eu/project/rcn/216008/en

[2] Funke H. W., Boerner S, Keinz J, et al. (2013). Experimental and Numerical Characterization of the Dry Low NOx Micromix Hydrogen Combustion Principle at Increased Energy Density for Industrial Hydrogen Gas Turbine Applications. In Turbo Expo: Power for Land, Sea, and Air (Vol. 55102, p. V01AT04A055). American Society of Mechanical Engineers.

[3] Funke H H W, Keinz J, Kusterer K, et al. (2017). Development and testing of a low NOx micromix combustion chamber for an industrial gas turbine. Int. J. Gas Turbine, Propuls. Power Syst, 9(1), 27-36.

[4] Sun X, Agarwal P, Carbonara F, Abbott D et al. (2020). Numerical Investigation into the Impact of Injector

Geometrical Design Parameters on Hydrogen Micromix Combustion Characteristics. Proceedings of the ASME Turbo Expo 2020: Turbomachinery Technical Conference and Exposition. GT2020-16084.

[5] Agarwal P, Sun X, Gauthier P Q and Sethi V. (2019). Injector Design Space Exploration for an Ultra-Low NOx Hydrogen Micromix Combustion System. In Turbo Expo: Power for Land, Sea, and Air (Vol. 58608, p. V003T03A013). American Society of Mechanical Engineers.

[6] Ghirardo G, Juniper MP, Bothien MR. (2018). The effect of the flame phase on thermoacoustic instabilities. Combustion and Flame, 187, 165-184.

[7] EASA. (2019) 'Type-certificate data sheet for Trent 1000 series engines', (April), pp. 1–32. Available at: https://www.easa.europa.eu/sites/default/files/dfu/TCDS E 036 issue 15.pdf

[8] Nikolaidis T, (2015) 'The Turbomatch Scheme'. Cranfield University.

[9] Walsh P P and Fletcher P. (2004). Gas Turbine Performance. Second Edi. Edited by Blackwell Pub.

[10] Adeniyi A A. (2015). A coupled Lagrangian-Eulerian framework to model droplet to film interaction with heat transfer. PhD thesis, University of Nottingham.

[11] Mellor A M. (1990). Design of Modern Turbine Combustors. Edited by P. Academic.

[12] Mattingly J D, Heisern W H and Pratt D T. (2002). Engine Component Design: Combustion Systems, in Aircraft Engine Design. Second Edi, pp. 325–418. doi: 10.2514/5.9781600861444.0325.0418.

[13] Poinsot T, (2017). Prediction and control of combustion instabilities in real engines. Proceedings of the Combustion Institute, 36(1), 1-28.

[14] Andreini A, Facchini B, Giusti A and Turrini F. (2014). Assessment of flame transfer function formulations for the thermoacoustic analysis of lean burn aero-engine combustors. Energy Procedia, 45(0), 1422-1431.

[15] Han X, Li J, Morgans A. (2015). Prediction of combustion instability limit cycle oscillations by combining flame describing function simulations with a thermoacoustic network model. Combustion and Flame, 162(10), 3632-3647.

[16] OSCILOS website: http://www.oscilos.com/, code and documentation available for download.

[17] McClure J, Abbott D, Agarwal P, et al. (2019). Comparison of Hydrogen Micromix Flame Transfer Functions Determined Using RANS and LES. In Turbo Expo: Power for Land, Sea, and Air (Vol. 58608, p. V003T03A009). American Society of Mechanical Engineers.

[18] Crocco L. (1951). Aspects of combustion stability in liquid propellant rocket motors part I: fundamentals. low frequency instability with monopropellants. Journal of the American Rocket Society, 21(6), 163-178.

[19] Sattelmayer T. (2003). Influence of the combustor aerodynamics on combustion instabilities from equivalence ratio fluctuations. J. Eng. Gas Turbines Power, 125(1), 11-19.

[20] Eckstein J, Sattelmayer T. (2006). Low-order modeling of low-frequency combustion instabilities in aeroengines. Journal of propulsion and power, 22(2), 425-432.

[21] Cheung W S, Sims G J M, Copplestone R W, Tilston J R, Wilson C W, Stow S R. and Dowling, A P. (2003). Measurement and analysis of flame transfer function in a sector combustor under high pressure conditions. In Turbo Expo: Power for Land, Sea, and Air (Vol. 36851, pp. 187-194).

[22] Li J, Yang D, Luzzato C and Morgans A S. (2017). Open Source Combustion Instability Low Order Simulator (OSCILOS-Long) Technical report, available for download on http://www.oscilos.com/

[23] Lòpez-Juàrez M, Sun X, Sethi B, Gauthier P and Abbott D. (2020). Characterising hydrogen micromix flames: combustion model calibration and evaluation. Proceedings of the ASME Turbo Expo 2020: Turbomachinery Technical Conference and Exposition. GT2020-14893.

[24] Paschereit C, Flohr P, Schuermans B, Prediction of combustion oscillations in gas turbine combustors, 39th Aerospace Sciences Meeting and Exhibit (2001), AIAAA Paper 2001-0484.

[25] Krebs W, Flohr P, Prade B, Hoffmann S, Thermoacoustic stability chart for high intensity gas turbine combustion systems, Combust. Sci. and Tech., 174 (7): pp. 99–128, 2002.

[26] Campa G, Camporeale S M, Prediction of the Thermoacoustic Combustion Instabilities in Practical Annular Combustors, Journal of Engineering for Gas Turbines and Power September 2014, Vol. 136 2014.

[27] Sun, X, Abbott, G, Singh A V, Gauthier P, Sethi, V. (submitted for publication). Numerical investigation of potential cause of instabilities in a hydrogen micromix injector array, Submitted for publication in Proceedings of ASME Turbo Expo 2021.

2021-09-16

Thermoacoustic behaviour of a hydrogen micromix aviation gas turbine combustor under typical flight conditions

Abbott, David

American Society of Mechanical Engineers

Abbott D, Giannotta A, Sun X, et al., (2021) Thermoacoustic behaviour of a hydrogen micromix aviation gas turbine combustor under typical flight conditions. In: ASME Turbo Expo 2021: Turbomachinery Technical Conference and Exposition, 7-11 June 2021, Virtual Event

https://doi.org/10.1115/GT2021-59844